

A Carbon Nanotube Based Nanorelay

J. M. Kinaret, T. Nord and S. Viefers

*Department of Applied Physics, Chalmers University of Technology
and Göteborg University, SE-412 96 Göteborg, Sweden*

(November 13, 2018)

We investigate the operational characteristics of a nanorelay based on a conducting carbon nanotube placed on a terrace in a silicon substrate. The nanorelay is a three terminal device that acts as a switch in the GHz regime. Potential applications include logic devices, memory elements, pulse generators, and current or voltage amplifiers.

Nanoelectromechanical systems (NEMS) are a rapidly growing research field with substantial potential for future applications. The basic operating principle underlying NEMS is the strong electromechanical coupling in nanometer-size electronic devices in which the Coulomb forces associated with device operation are comparable with the chemical forces that hold the devices together. Carbon nanotubes (CNT)¹ are ideal candidates for nanoelectromechanical devices due to their well-characterized chemical and physical structures, low masses, exceptional directional stiffness, and good reproducibility. Nanotube-based NEMS have internal operating frequencies in the gigahertz range, which makes them attractive for a number of applications. Recent progress in this direction includes fabrication of CNT nanotweezers,^{2,3} CNT based random access memory,⁴ and super-sensitive sensors.^{5,6}

In this paper we consider another example of CNT based NEMS, a so-called nanorelay. This three-terminal device consists of a conducting CNT placed on a terraced Si substrate and connected to a fixed source electrode. A gate electrode is positioned underneath the CNT so that charge can be induced in the CNT by applying a gate voltage. The resulting capacitive force between the CNT and the gate bends the tube and brings the tube end into contact with a drain electrode on the lower terrace, thereby closing an electric circuit. We describe the system with a model based on classical elasticity theory⁷ and the orthodox theory of Coulomb blockade,^{8,9} and study its IV-characteristics and switching dynamics. Theoretical studies of a related two-terminal structure have recently been reported.^{10,11}

Model system. The geometry of the nanorelay is depicted in Fig. 1. We model the CNT as an elastic cantilever using continuum elasticity theory:⁷ Assuming that only the lowest vibrational eigenmode is excited, and that the bending profile upon applying an external force is the same as that of free oscillations, one can express the potential energy of the bent tube in terms of the deflection x of its tip as $V = kx^2/2$. The effective spring constant k depends on the geometry of the tube and is approximately given by $k \approx 3EI/L^3$. Here E is Young's modulus, experimentally determined to be approximately 1.2 TPa,^{12,13} L is the tube length and $I = \pi(D_o^4 - D_i^4)/64$ its moment of inertia, D_o and D_i being the outer and inner diameters of the (multi-

walled) CNT. The effective mass of the tube is $m_{eff} = k/\Omega^2 \approx 3M/(1.875)^2$, where M is the total tube mass and Ω its lowest eigenfrequency.⁷ It is known experimentally that Q-factors of CNT cantilevers are of the order of 170-500.¹⁴ We model this by a phenomenological damping force $-\gamma_d \dot{x}$ in the equations of motion.

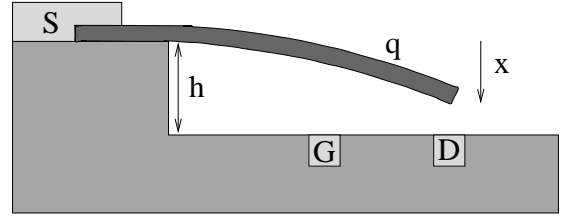


FIG. 1. Schematic picture of the model system consisting of a conducting carbon nanotube placed on a terraced Si substrate. The terrace height is labeled h , and q denotes the excess charge on the tube. The CNT is connected to a source electrode (S), and the gate (G) and drain (D) electrodes are placed on the substrate beneath the CNT at lengths L and L_G away from the terrace. The displacement x of the nanotube tip is measured towards the substrate. Typically, $L \approx 50 - 100$ nm, $h \approx 5$ nm.

For a metallic nanotube, the effective impedance Z is dominated by the contact resistance at the source contact and is mostly ohmic. If a gate voltage is applied, the resulting capacitive force bends the tube so that a tunneling current can flow to drain, whereas due to the long tube-gate distance no electrons tunnel between the tube and the gate electrode. Finite element calculations show that the drain- and gate capacitances are well approximated by those of parallel plate capacitors.¹⁵ We thus model them as

$$\begin{aligned} C_d(x) &= \frac{C_0}{1 - \frac{x}{h}(1 - C_0/C_h)}, \\ C_g(x) &= \frac{2C_0}{1 - \kappa \frac{x}{h}(1 - C_0/C_h)}. \end{aligned} \quad (1)$$

Here $C_0 \equiv C_d(x = 0)$ is the drain capacitance for a

horizontal tube and $C_h \equiv C_d(x = h)$ is that for the tube in contact with the drain electrode. The latter can be estimated from experiments.¹⁶ The constant κ ($0 < \kappa < 1$) accounts for the fact that the deflection at the position of the gate is smaller than that of the tip. The corresponding capacitive forces take the form $F_c = -(Q^2/2)\nabla(1/C(x))$.

The tunneling resistance is modeled as $R_T = R_0 \exp[(h-x)/\lambda]$, where the tunneling length λ depends on the contact material and is typically of the order of 0.5 Å, and R_0 is estimated from experimental results.¹⁶ Following Ingold and Nazarov⁹ for the case of zero temperature and an ohmic environmental impedance Z , we determine the tunneling rate at a given deflection x and source-drain voltage V_{sd} as

$$\Gamma(x) = \frac{1}{e^2 R_T(x)} \int_0^{eV} dE P(E) (eV - E) \quad (2)$$

where $P(E)$, the probability for energy exchange between the tunneling electron and the environment, is determined self-consistently from

$$EP(E) = \frac{2}{g} \int_0^E dE' \left[1 + \frac{\pi}{g} \left(\frac{E - E'}{E_c(x)} \right)^2 \right]^{-1} P(E'). \quad (3)$$

Here, $E_c(x) = e^2/(2C(x))$ and $g = R_K/Z$ where $R_K = h/e^2 \approx 25.8$ kΩ is the von Klitzing constant.

The above model results in a set of coupled non-linear differential equations describing both the mechanical motion and the current flow in the system,

$$m_{eff} \ddot{x}(t) = -kx(t) - \gamma_d \dot{x}(t) + F_{c,gate} + F_{c,drain} + F_{contact} \quad (4)$$

$$Z\dot{q}(t) = -\frac{q(t) + V_g C_g(x)}{C_g(x) + C_d(x)} + V_s - ZI_t(t) \quad (5)$$

where I_t is the stochastic tunneling current, and the zero of the potential has been chosen such that $V_d = 0$. The contact force $F_{contact}$ represents the short range forces between the tube tip and the drain electrode important at large deflections; presently, we model the surface interactions as elastic collisions. For a set of applied voltages, design parameters and initial conditions, we solve the equations of motion numerically using a fourth order Runge-Kutta method. The tunneling probability is computed at every time step, and tunneling events are treated as a (weighted) random process (for algorithmic details, see Ref. 17).

Results. In our simulations we have studied the dc IV-characteristics of the nanorelay and its response $I_d(t)$ to a gate voltage pulse. Fig. 2 shows the drain current as a function of gate- and source-drain voltages. Due to the exponential dependence of the tunneling resistance on tube deflection, there is a sharp transition from a non-conducting (OFF) to a conducting (ON) state when the gate voltage is varied at fixed source-drain voltage. The

sharp switching curve allows for amplification of weak signals superimposed on the gate voltage; detailed analysis of the amplification characteristics will be pursued elsewhere. The inset shows a high resolution plot of the drain current as a function of V_{sg} for various V_{sd} , and demonstrates that the pull-in voltage V_{sg}^* depends weakly on V_{sd} as expected, giving rise to highly non-linear $I_d(V_{sd})$ characteristics near the transition.

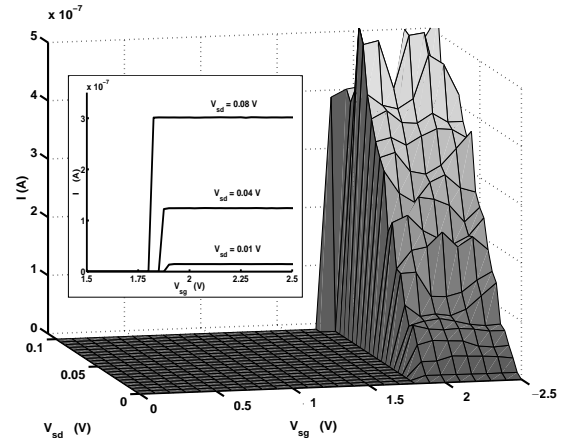


FIG. 2. Drain current as a function of source-drain voltage and gate voltage. The parameters used here are $L = 75$ nm, $h = 3$ nm, $D_i = 2$ nm, $D_o = 3$ nm, $L_G = 0.7L$ and $Z = 8$ kΩ. The pull-in voltage V_{sg}^* for various values of V_{sd} can be read off the higher resolution IV curves shown in the inset.

For certain choices of parameters, hysteresis occurs in the OFF-ON-OFF transition. This is illustrated in Fig. 3 which shows I_d as a function of V_{sg} for up- and down-sweeps. The hysteresis is due to the appearance of two stable cantilever positions for certain design parameters and gate voltages: one of the stable positions is at contact (ON state) and the other is a slightly bent tube configuration ($x \lesssim h/2$) corresponding to an OFF state. The inset of Fig. 3 shows the contours of zero net force as a function of gate voltage and tube deflection (net force is positive to the right of the contour) for two sets of design parameters; hysteresis arises for the first set of parameters in a range of gate voltages when there are two zero force configurations. The amount of hysteresis can be controlled by device design — for example, placing the gate electrode further from the drain decreases hysteresis. The hysteretic switching characteristics may be utilized to construct nanotube-based nanoelectromechanical memory elements.

Finally, we studied the switching dynamics of the nanorelay, choosing a set of parameters for which hysteresis is unimportant. The simulation presented here started in the OFF state with $V_{sg} = 0$ V, switched to the ON state ($V_{sg} = 3$ V, see Fig. 2) at $t = 0.5 \mu s$ and back to $V_{sg} = 0$ V at $t = 1 \mu s$. The resulting switching times were

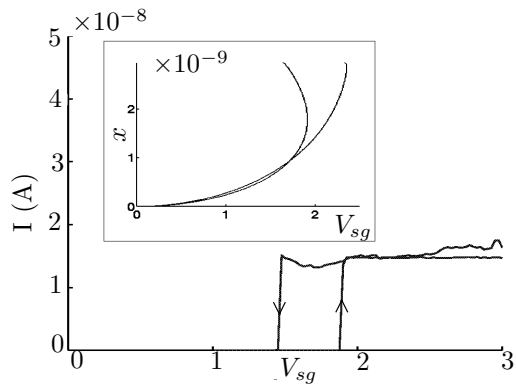


FIG. 3. Switching curves for up- and down-sweeps of V_{sg} for various V_{sd} showing hysteresis ($L = 75$ nm, $L_G = 0.7L$, $D_i = 2$ nm, $D_o = 3$ nm). Inset: contours of zero net force as a function of V_{sg} and cantilever deflection x for two devices (total force is positive to the right of each curve). The appearance of two configurations with zero net force for some V_{sg} gives rise to two stable cantilever positions corresponding to ON and OFF states, with associated hysteresis. Device showing hysteresis $L = 75$ nm, $L_G = 0.7L$, device without hysteresis $L = 100$ nm, $L_G = 0.5L$, other parameters as given above.

tens of nanoseconds for the OFF-ON transition (*e.g.* rise time $\tau_R \approx 20$ ns), while the ON-OFF transition was considerably faster (fall time $\tau_F \approx 0.1$ ns). This asymmetry is in part due to the large difference between the step height and the tunneling length, in part to the cantilever bouncing off the drain surface during the OFF-ON transition. The switching dynamics are quite sensitive to the geometrical parameters which means that they can be optimized for specific applications. The time constants also depend on the details of the surface force $F_{contact}$ which are beyond our model. In particular, the OFF-ON transition time is greatly reduced by dissipative surface processes (*e.g.* phonon emission) that dampen tube vibrations, and allow the CNT to settle faster at a stationary near-contact position.

The van der Waals (vdW)¹⁸ and adhesive¹⁹ forces between the CNT and the substrate were neglected in our model. Dequesnes *et al.*¹⁰ recently studied the effect of vdW forces on the pull-in voltage V_g^* for a two-terminal device (the entire substrate acting as a gate electrode). The main result is that vdW forces reduce the pull-in voltage, but do not change the qualitative features of the OFF-ON transition. Moreover, the significance of the vdW forces decreases with decreasing tube length and increasing terrace height or tube diameter, and their effect on V_g^* is negligible for a wide range of design parameters. Concerning the ON-OFF transition, adhesive forces¹⁹, enhance the tendency of the CNT to remain in contact even after the gate voltage has been switched off. We have performed a simple analysis comparing the magnitude of the adhesive forces (modeled by a Morse

potential) and vdW forces (based on a Lennard-Jones potential) to the mechanical and electrostatic ones, and find that the sticking problem can be avoided by a suitable choice of parameters such as shorter or thicker CNTs. Another effect we have neglected is the possibility of field emission,²⁰ which may play a role in the geometry considered in this paper. An investigation of these points will be the focus of a future publication.

In conclusion, we have performed a theoretical analysis of a CNT-based three-terminal nanoelectromechanical switch. The large parameter space for its design allows for a number of potential applications, such as amplifiers, logic devices or memory elements.

We would like to thank Torgny Johansson, Hans Hansson, Andreas Isacson, Herre van der Zant and Eleanor Campbell for useful discussions. We gratefully acknowledge financial support from the Foundation for Strategic Research through its program CAMEL (Carbon Allotropes for Microelectronics).

-
- ¹ R. Saito, G. Dresselhaus and M.S. Dresselhaus, *Physical Properties of Carbon Nanotubes*, (Imperial College Press, London, 1998).
 - ² P. Kim and C.M. Lieber, *Science* **286**, 2148 (1999).
 - ³ S. Akita, Y. Nakayama, S. Mizooka, Y. Takano, T. Okawa, Y. Miyatake, S. Yamanaka, M. Tsuji and T. Nosaka, *Appl. Phys. Lett.* **79**, 1691 (2001).
 - ⁴ T. Rueckes, K. Kim, E. Joselevich, G.Y. Tseng, C-L. Cheung and C.M. Lieber, *Science* **289**, 94 (2000).
 - ⁵ P.G. Collins, K.B. Bradley, M. Ishigami and A. Zettl, *Science* **287**, 1801 (2000).
 - ⁶ C.K.W. Adu, G.U. Sumanasekera, B.K. Pradhan, H.E. Romero and P.C. Eklund, *Chem. Phys. Lett.* **337**, 31 (2001).
 - ⁷ L.D. Landau and E.M. Lifschitz, *Lehrbuch der theoretischen Physik VII: Elastizitätstheorie* (Akademie Verlag, Berlin, 1975).
 - ⁸ I. O. Kulik and R. I. Shekhter, *Sov. Phys. JETP* **41**, 308 (1975).
 - ⁹ G. L. Ingold and Y. N. Nazarov, in *Single Charge Tunneling, NATO ASI*, edited by M. H. Devoret and H. Grabert (Plenum Press, New York, 1992).
 - ¹⁰ M. Dequesnes, S.V. Rotkin and N.R. Aluru, *Nanotechnology* **13**, 120 (2002).
 - ¹¹ K.A. Bulashevich and S.V. Rotkin, *JETP Letters* **75**, 205 (2002).
 - ¹² M.M. Treacy, T.W. Ebbesen and J.M. Gibson, *Nature* **381**, 678 (1996).
 - ¹³ E.W. Wong, P.E. Sheehan and C.M. Lieber, *Science* **277**, 1971 (1997).
 - ¹⁴ P. Poncharal, Z. L. Wang, D. Ugarte and W. A. de Heer, *Science* **283**, 1513 (1999).

- ¹⁵ T. Johansson, M. Sc. Thesis, Chalmers University of Technology (2001).
- ¹⁶ R. Tarkiainen, M. Ahlskog, J. Penttilä, L. Roschier, P. Hakonen, M. Paalanen and E. Sonin, Phys. Rev. B **64**, 195412 (2001).
- ¹⁷ A. Isacson, Ph.D. thesis, Chalmers University of Technology (2002).
- ¹⁸ J.N. Israelachvili, *Intermolecular and Surface Forces* (Academic Press, London, 1985).
- ¹⁹ C.J. Chen, J. Phys.: Condens. Matter **3**, 1227 (1991).
- ²⁰ J.-M. Bonard, H. Kind, T. Stöckli and L.-O. Nilsson, Solid State Electronics **45**, 893 (2001).